Neuroradiology

The Essentials with MR and CT

Second Edition

Val M. Runge

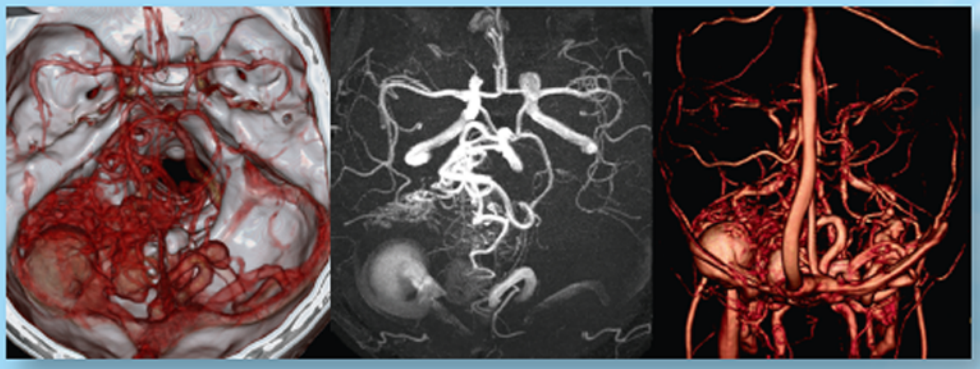

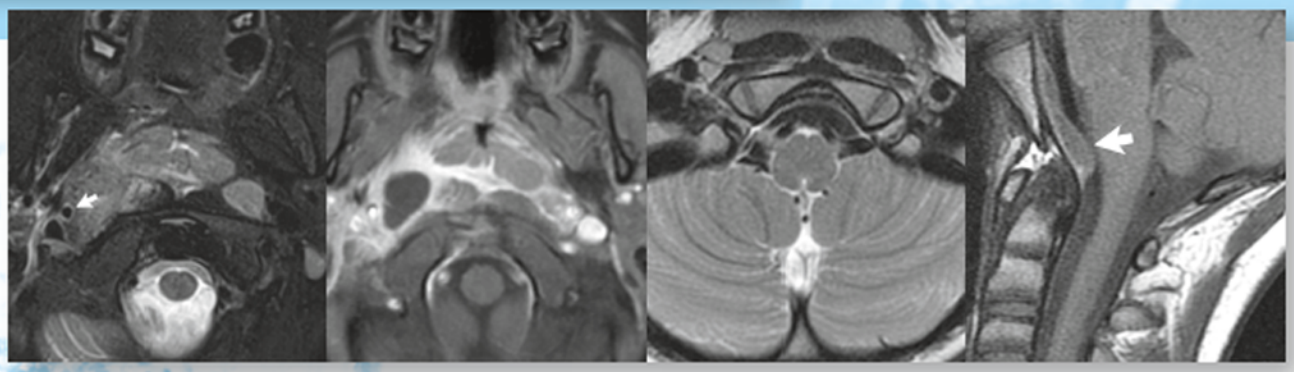

Thieme


Thieme

Neuroradiology

The Essentials with MR and CT

Second Edition

Val M. Runge, MD
Professor
Department of Diagnostic, Interventional, and Pediatric Radiology
University Hospital of Bern, Inselspital
University of Bern
Bern, Switzerland

1328 illustrations

Thieme
New York • Stuttgart • Delhi • Rio de Janeiro

Library of Congress Cataloging-in-Publication Data is available from the publisher.

Thieme Publishers New York
333 Seventh Avenue, New York, NY 10001 USA
+1 800 782 3488, customerservice@thieme.com

Georg Thieme Verlag KG
Rüdigerstrasse 14, 70469 Stuttgart, Germany
+49 [0]711 8931 421, customerservice@thieme.de

Thieme Publishers Delhi
A-12, Second Floor, Sector-2, Noida-201301
Uttar Pradesh, India
+91 120 45 566 00, customerservice@thieme.in

Thieme Publishers Rio de Janeiro,
Thieme Publicações Ltda.
Edifício Rodolpho de Paoli, 25º andar
Av. Nilo Peçanha, 50 – Sala 2508
Rio de Janeiro 20020-906 Brasil
+55 21 3172 2297

Cover design: Thieme Publishing Group
Typesetting by DiTech Process Solutions, India

Printed in USA by King Printing Company, Inc. 5 4 3 2 1

ISBN 978-1-68420-153-2

Also available as an e-book:
eISBN 978-1-68420-154-9

Contents

Foreword

From the first edition

Drs. Runge, Smoker, and Valavanis and their collaborators have done a superb job of distilling the essential aspects of Neuroradiology into a compact textbook. This book has a higher image to text ratio than most books I have read, making it the perfect companion for the neuroradiology PACS workstation. It should be required reading for residents prior to a neuroradiology rotation and for neuroradiology fellows before they begin their fellowship. However, it is so complete and image-rich that I plan to flip through the pages before the next time I sit for the Neuroradiology Certificate of Additional Qualification (CAQ) exam. It will also be of interest to neurology and neurosurgical trainees and attendings as an excellent review of the MRI and CT studies they encounter every day on their patients. *Neuroradiology: The Essentials with MR and CT* really covers the subspecialty from soup to nuts, from normal anatomy to disease, from the routine (e.g., stroke and multiple sclerosis) to cases that might only be seen once a year (e.g., glutaric acidemia type 1 and CADASIL). The image quality is excellent and the images are quite representative of what would normally be encountered in academic or community practice. The reader will note that there is a modicum of relevant MR physics interleaved in the discussion. This is reminiscent of Dr. Runge's previous MR physics textbooks. Since I believe this is Dr. Runge's sixteenth book, one expected clear, concise explanations of both MR physics and clinical neuroradiology and that's indeed the case. As noted above, this book should have a place next to the Neuroradiology PACS workstation for ready reference when one "just wants to be sure" or to flesh out the clinical aspects of the imaging findings for discussion with our clinical neuroradiology colleagues. However, I would be sure to bolt this book down because I suspect it will have a high tendency to "walk." I hope you enjoy reading it as much as I did.

William G. Bradley Jr., MD, PhD, FACR
Former Professor and Chairman, Department of Radiology
University of California San Diego
San Diego, California

Preface

Neuroradiology: The Essentials with MR and CT, Second Edition is written both to be read from cover to cover and to be used as a quick reference in the midst of a busy clinical day. The second edition adds many new figures, includes updates concerning 7T, and provides greater text detail particularly concerning brain aneurysms and AVMs. Designed as a practical educational resource for clinical neuroradiology, the text is divided into three sections: the brain, head and neck, and spine. Care has been taken for the text to be inclusive, yet focused on commonly encountered diseases, and to cover well the breadth of the field without gaps.

The diseases and their imaging presentations that one is likely to encounter in clinical practice, and which are essential to know, are included. The focus is on illustrating and describing the MR and CT appearances of these, discussing in depth the imaging findings. The text is written from a clinical radiology perspective, drawing on personal experience and covering common imaging findings often not well described in more traditional, academic textbooks.

The true basis of the text is that of clinical neuroradiology—that is, recognition of characteristic findings on both MR and CT of the disease processes we are likely to encounter in clinical practice, using as a basis excellent images and case materials from both modalities.

Val M. Runge, MD

Abbreviations

The following abbreviations are used with the figures, to enable rapid recognition of imaging technique and to permit the legends to be more concise.

ADC	Apparent diffusion coefficient
ASL	Arterial spin labeling
CBF	Cerebral blood flow
CBV	Cerebral blood volume
CE CT	Contrast-enhanced computed tomography
CE MRA	Contrast-enhanced magnetic resonance angiography
CE T1	Contrast-enhanced T1-weighted
CE T1 FS	Contrast-enhanced T1-weighted, with fat suppression
CT	Computed tomography
CTA	Computed tomography angiography
DSA	Digital subtraction angiography
DWI	Diffusion weighted imaging
FLAIR	Fluid attenuated inversion recovery
GRE	Gradient recalled echo, specifically with T2* weighting
MTT	Mean transit time
PD	Proton density weighted
PET	Positron emission tomography
STIR	Short tau inversion recovery
T1	T1-weighted
T1 FS	T1-weighted, with fat suppression
T2	T2-weighted
T2 FS	T2-weighted, with fat suppression
TOF	Time of flight magnetic resonance angiography
TTP	Time to peak

Acknowledgments

Some figures and text have been excerpted with permission from the following Thieme publications: *The Physics of Clinical MR Taught Through Images*, 4th edition; *Essentials of Clinical MR; Clinical 3T Magnetic Resonance*; and *Imaging of Cerebrovascular Disease*. A small number of figures, together with some source text, were also used from the following publication, for which Val M. Runge is the sole editor/author and who also owns the copyright: *Clinical Magnetic Resonance Imaging.*

1 Brain

1.1 Normal Anatomy and Common Variants

1.1.1 Normal Intracranial Anatomy

The frontal lobe is demarcated posteriorly from the parietal lobe by the central sulcus (▶ Fig. 1.1). On axial magnetic resonance (MR) images near the vertex, the central sulcus is readily identified. It is the major sulcus just behind the "L," the intersection of two sulci formed in part by the superior frontal sulcus. The precentral gyrus lies just anterior to the central sulcus and the postcentral gyrus just posteriorly. As a generalization, the primary motor area (Brodmann area 4) is located in the precentral gyrus, and the primary somatesthetic (body's sensations) area (Brodmann areas 1, 2, and 3) in the postcentral gyrus. The parietal lobe is demarcated from the occipital lobe posteriorly by the parieto-occipital sulcus (fissure). The anatomy of the nuclei and white matter tracts is beyond the scope of this book, but see ▶ Fig. 1.2. The reader is referred to the many computer-based atlases, including *The Human Brain in 1969 Pieces* by Wieslaw Nowinski.

The pituitary gland is divided into anterior and posterior lobes. The anterior pituitary is referred to as the adenohypophysis and the posterior pituitary as the neurohypophysis. The normal

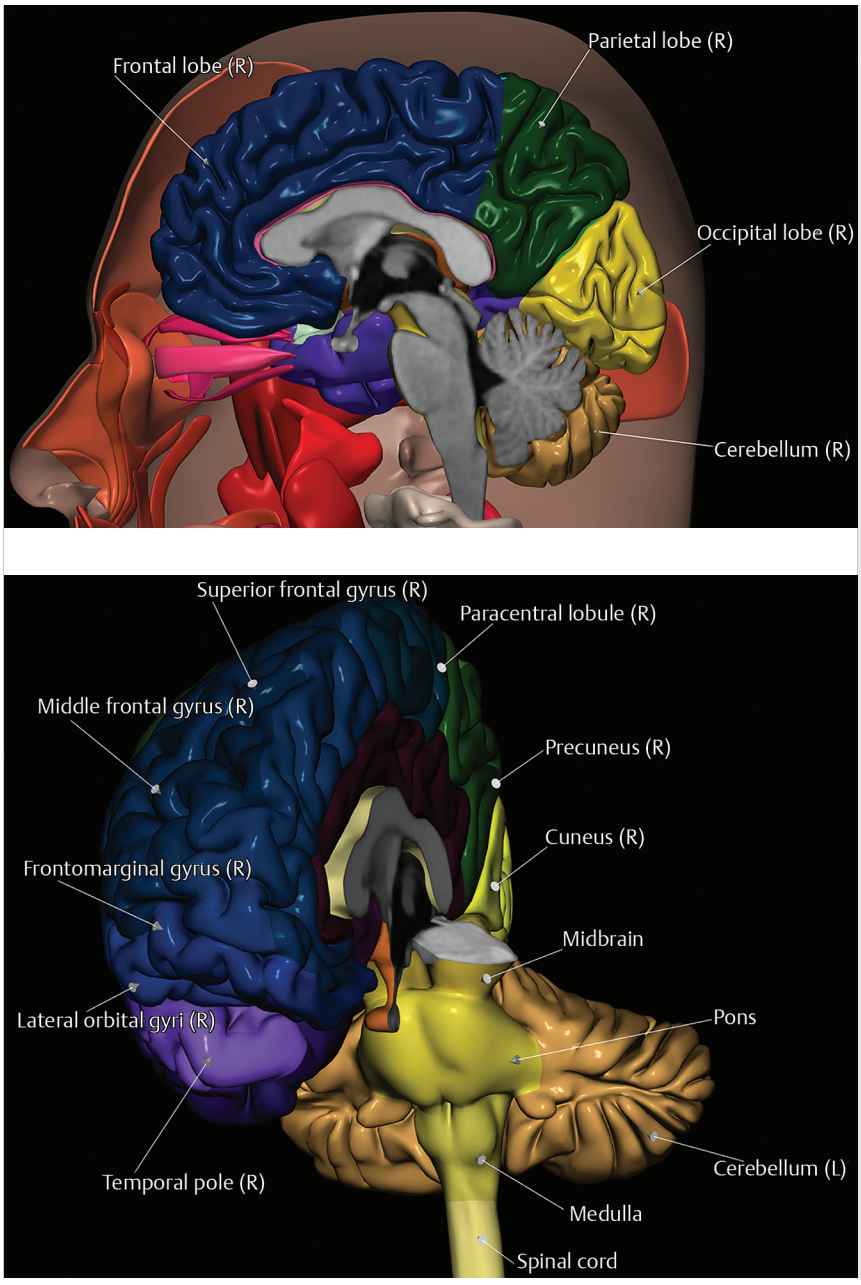

Fig. 1.1 Normal lobar and gyral anatomy. Important landmarks include the central sulcus, which separates the frontal lobe anteriorly from the parietal lobe posteriorly, and the sylvian fissure (the lateral sulcus), which divides the frontal and parietal lobes above from the temporal lobe below. The parietal and occipital lobes are separated by the parietooccipital sulcus. (Courtesy of Wieslaw Nowinski, DSc, PhD.)

(*Continued*)

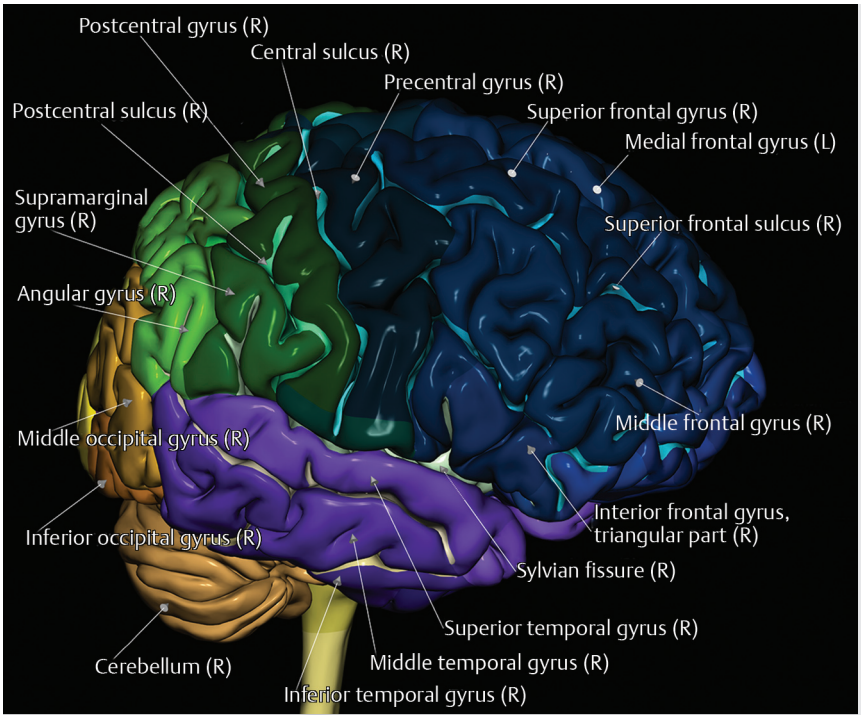

Fig. 1.1 (*Continued*)

pituitary is less than 10 mm in height, and demonstrates intense enhancement following intravenous contrast administration, due to the lack of a blood-brain barrier. A common variant in appearance of the pituitary is a slight upward convex superior margin, which can be seen in young women. On T1-weighted scans, the posterior pituitary is seen to be hyperintense in up to half of the normal patient population, a finding that is more common in younger patients (but not in the elderly).

The internal auditory canal (IAC) is a bony foramen within the petrous portion of the temporal bone. It contains the 7th (facial) and 8th (vestibulocochlear) nerve complexes. The 7th nerve lies in the anterior superior quadrant of the IAC, when viewed in cross-section, and runs laterally to the geniculate ganglion. The cochlear division of the 8th nerve lies in the anterior inferior quadrant. The superior and inferior vestibular nerves, also divisions of the 8th nerve, which supply information concerning equilibrium, lie in the superior and inferior posterior quadrants. As visualized in the axial plane, the cochlea is anterior and the vestibule posterior. There are three semicircular canals: the lateral (which has a horizontal orientation), superior, and posterior. The fluid (endolymph) within the cochlea, vestibule, and semicircular canals is normally isointense to cerebrospinal fluid (CSF) on MR.

1.1.2 Normal Arterial Anatomy

Three major arteries supply the cerebral hemispheres (▶ Fig. 1.3). The anterior cerebral artery (ACA) supplies the anterior two-thirds of the medial cerebral surface and 1 cm of superior medial brain over the convexity. The recurrent artery of Heubner, which originates from the A1 or A2 segment of the ACA, supplies the caudate head, anterior limb of the internal capsule, and part of the putamen. The posterior limb of the internal capsule, portions of the thalamus, the caudate, the globus pallidus, and the cerebral peduncle are supplied by the anterior choroidal artery, which arises from the supraclinoid internal carotid artery. The middle cerebral artery (MCA) supplies the lateral portion of the cerebral hemispheres, the insula, and the anterior and lateral temporal lobes. The lenticulostriate arteries, which originate from the M1 segment of the MCA, supply the lentiform nucleus (globus pallidus and putamen) and the anterior limb of the internal capsule. The posterior cerebral artery (PCA) supplies the occipital lobe and the medial temporal lobe. The thalamoperforating and thalamogeniculate branches supply the medial portion of the thalami and the walls of the third ventricle. These small perforating branches arise from the P1 segment of the PCA with similar branches arising from the posterior communicating artery (▶ Fig. 1.4).

Three major but smaller vessels supply the cerebellum (▶ Fig. 1.5). The largest is the posterior inferior cerebellar artery (PICA), which supplies the tonsil, the inferior vermis, and the inferior cerebellum (with the exception of its most anterior extent). The anterior inferior cerebellar artery (AICA) supplies the anterior inferior portion of the cerebellum and is the smallest of the three vessels. It is commonly stated that the distribution of AICA is in continuum with PICA, with at times the distribution slightly larger or smaller. The superior cerebellar artery supplies the superior half of the cerebellum.

The circle of Willis is complete in only one quarter of the population. Variants include the following. A fetal origin of the posterior cerebral artery, with its origin from the internal carotid artery instead of the basilar artery, is seen in about one in five patients. The P1 segment of the posterior cerebral artery, which is the portion from the tip of the basilar artery to the junction with the posterior communicating artery (PCOM), is usually also hypoplastic in this circumstance. The PCOM is hypoplastic in one-third of patients. The anterior communicating artery (ACOM), which connects the two anterior cerebral arteries, is hypoplastic

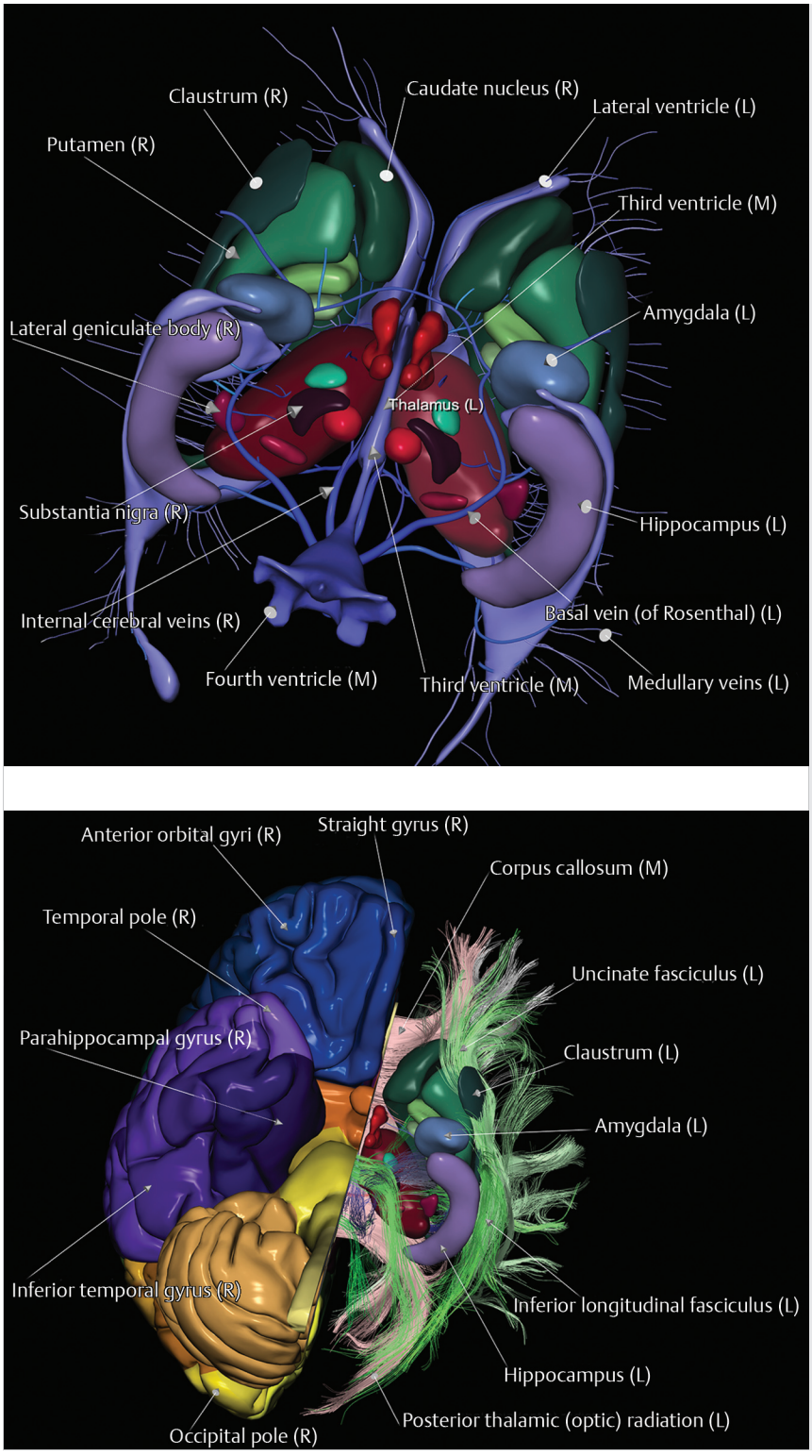

Fig. 1.2 Brain nuclei and white matter tracts, normal anatomy. Most relevant to MR interpretation are the locations of the caudate nucleus, putamen, globus pallidus (*light green,* immediately medial to the putamen and not labeled), hippocampus, and thalamus. Note also the location of the optic radiations. (Courtesy of Wieslaw Nowinski, DSc, PhD.)

in 15%. The A1 segment of the anterior cerebral artery, which begins at the carotid terminus and continues to the juncture with the ACOM, is hypoplastic in 10%.

The external carotid artery is the smaller of the two terminal branches of the common carotid artery. It arises anterior and medial to the internal carotid artery, then courses posterior laterally. There are many muscular branches, with the early branching of the external carotid artery allowing rapid recognition of this vessel in distinction to the internal carotid artery.

The internal carotid artery was traditionally divided into four major segments: the cervical, the petrous (horizontal), the cavernous (juxtasellar), and the intracranial (supraclinoid) portions. Today, there are seven recognized segments (C1 to C7): the cervical, petrous, lacerum, cavernous, clinoid, ophthalmic, and

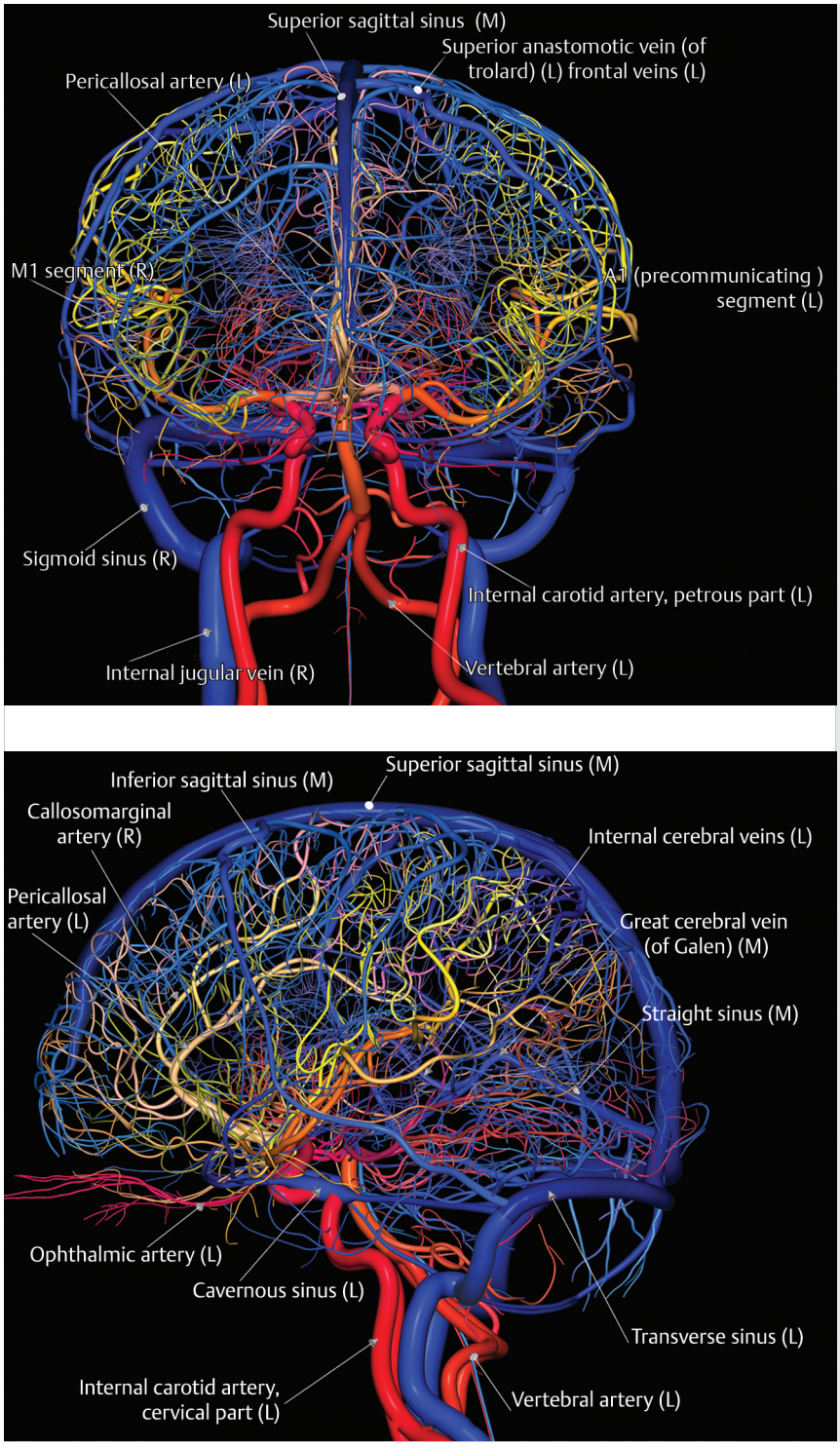

Fig. 1.3 Normal arterial and venous anatomy. Anteroposterior and lateral projections are illustrated. (Courtesy of Wieslaw Nowinski, DSc, PhD.)

communicating (terminal) segments. At its origin, the internal carotid artery is somewhat dilated, forming the carotid bulb. The petrous segment, C2, of the internal carotid artery has three sections: the ascending (vertical), the genu (bend), and the horizontal portions. The lacerum segment, C3, is still extradural. The cavernous segment, C4, is surrounded by the cavernous sinus. The meningohypophyseal artery arises from C4. The clinoid segment, C5, is very short, and begins after the artery exits from the cavernous sinus. C5 extends from the proximal dural ring to the distal dural ring. C6, the ophthalmic segment, extends from the distal dural ring (with this portion of the internal carotid artery thus considered intradural) to the origin of the PCOM. The ophthalmic artery arises from C6. C7 is that segment of the artery extending from the origin of the posterior communicating artery to the carotid terminus, where the vessel divides into the anterior and middle cerebral arteries. C6 and C7 together constitute the supraclinoid internal carotid artery.

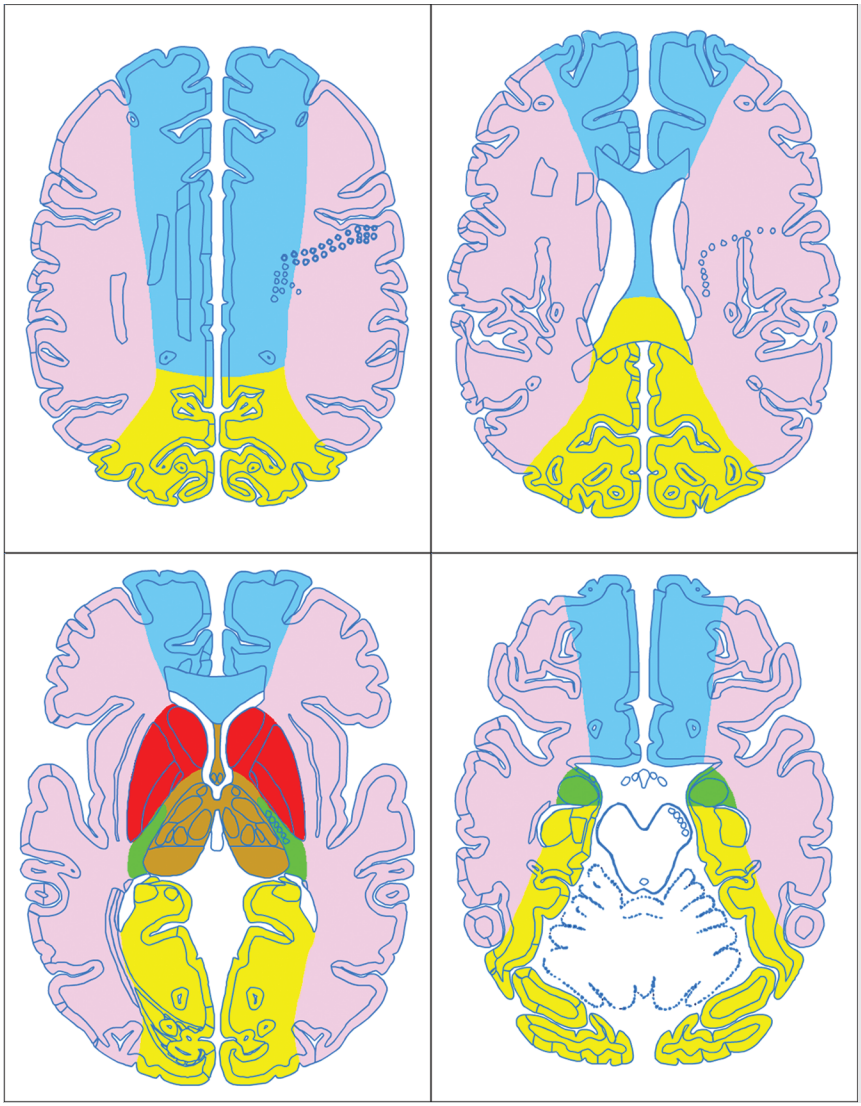

Fig. 1.4 Supratentorial arterial territories. Axial diagrams of the brain at four levels depict the major arterial territories of the supratentorial region, specifically the anterior cerebral artery (*blue*), middle cerebral artery (*pink*), and posterior cerebral artery (*yellow*) territories. In *red* is the vascular territory supplied by the penetrating branches of the middle cerebral artery (the lenticulostriate arteries). In *brown* is the territory supplied by the penetrating branches of the posterior cerebral arteries (the posterior thalamoperforators) and posterior communicating arteries (the anterior thalamoperforators). In *green* is the territory supplied by the anterior choroidal artery, which supplies amongst other structures the posterior limb of the internal capsule, the optic tract, and the hippocampus and amygdala. (Courtesy of Wieslaw Nowinski, DSc, PhD.)

There are many extracranial-intracranial vascular anastomoses. Two of these involve the ophthalmic artery. There are also multiple internal carotid-vertebral artery anastomoses, which represent persistent embryonic circulatory patterns. One of these is seen not uncommonly, as a normal variant, and is the persistent trigeminal artery (▶ Fig. 1.6). Pialleptomeningeal anastomoses are also present, and are an important potential source of collateral blood flow in occlusive vascular disease.

1.1.3 Normal Venous Anatomy

Regarding the central venous anatomy of the brain, the paired internal cerebral veins and basal veins of Rosenthal join to form the vein of Galen. The latter is then joined by the inferior sagittal sinus, which lies along the free edge of the falx, to form the straight sinus, which drains to the confluence of the sinuses (torcular herophili). Superficial cerebral veins over the convexity join to form the superior sagittal sinus, which lies along the midline, which then drains to the confluence of the sinuses. Flow continues via the transverse sinuses, which are often asymmetric (with the right usually dominant), to the sigmoid sinus, the jugular bulb, and then the internal jugular vein. There are three large named superficial veins. There is the superficial middle cerebral vein, which lies in the Sylvian fissure and drains into the cavernous or sphenoparietal sinus. The vein of Trolard joins the superior sagittal sinus and the superficial middle cerebral vein. The vein of Labbe joins the transverse sinus and the superficial middle cerebral vein. The venous system is currently best demonstrated (when considering computed tomography [CT] and MR) on two-dimensional (2D) time of flight (TOF) MR angiography.

1.1.4 Normal Myelination

Myelination begins in the brainstem, progresses to the cerebellum and cerebrum, with the order of myelination from central to peripheral, inferior to superior, and posterior to anterior. T1-weighted images are particularly useful to assess myelination in the first 9 months of life. With normal myelination, on T1-weighted images, white matter becomes higher in signal intensity. T2-weighted images are more useful to assess myelination after 6 months of age. However, it is important to note that longer repetition times (TRs) are required to evaluate the brain

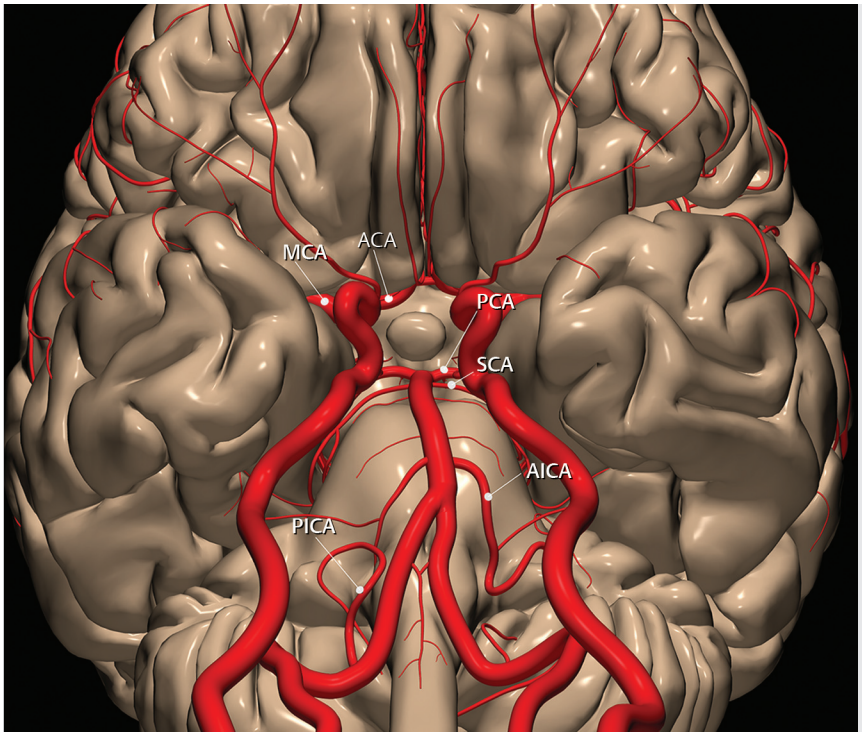

Fig. 1.5 Arterial supply of the posterior circulation, visualized on an anatomic drawing of the base of the brain. The posterior inferior cerebellar artery (PICA) originates from the vertebral artery. The two vertebral arteries join to form the basilar artery, with the major paired branches (in order from caudal to cranial) being the anterior inferior cerebellar artery (AICA), the superior cerebellar artery (SCA), and the posterior cerebral artery (PCA)—the latter marking the termination of the basilar artery. (Courtesy of Wieslaw Nowinski, DSc, PhD.)

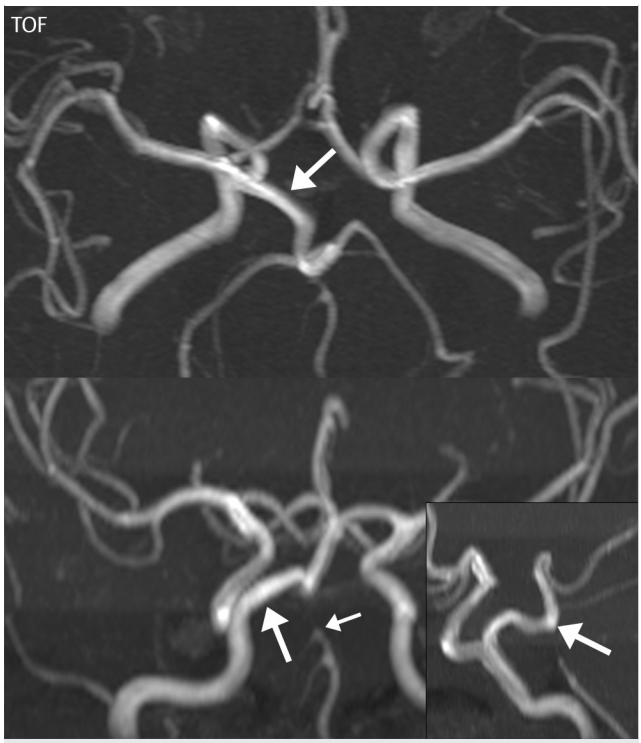

Fig. 1.6 Persistent trigeminal artery. Three projections from a 3D time-of-flight MRA of the circle of Willis are presented. The proximal basilar artery is small, and terminates in its mid-section (*small arrow*). The distal basilar artery is supplied from the right internal carotid artery, via a persistent embryonic connection (*large arrow*).

under 2 years of age (with T2-weighted scans), when compared to the adult. On T2-weighted images, with normal myelination, white matter becomes lower in signal intensity. This is due to the lower water content as myelin matures.

Myelination is quite specific for age from the newborn to 2 years of life; however, for simplification, the normal appearance is discussed at only four time frames. The dorsal pons, superior and inferior cerebellar peduncles, posterior limb of the internal capsule, and ventral lateral thalamus will demonstrate partial myelination, best seen on T1-weighted scans, in the newborn (▶ Fig. 1.7). The corpus callosum at this time is not myelinated, and will also appear thin.

At 6 months of age, on T1-weighted scans, the white matter of the cerebellum, the anterior limb and genu of the internal capsule, the white matter of the occipital lobe, and the posterior centrum semiovale will all appear normally myelinated with high signal intensity. The corpus callosum at this age will be partially myelinated, but will also still appear to be thin. At 6 months of age, on T2-weighted scans, only the posterior limb of the internal capsule will demonstrate low signal intensity, indicative of myelination.

At 12 months of age, on a T1-weighted scan, there will be a near adult pattern of myelination, specifically seen both in the deep and peripheral white matter. This pattern is reached by 9 months of age. On a T2-weighted scan, the deep white matter, specifically the internal capsule, corpus callosum, and corona radiata, will appear mature, with low signal intensity. Myelination is not yet complete at this age, as depicted on the T2-weighted scan, in the white matter of the frontal, temporal, parietal, and occipital lobes, together with the more peripheral subcortical white matter. These areas will still appear isointense to gray matter, not the low signal intensity (SI) on a T2-weighted scan indicative of mature myelination.

At 2 years of age, the deep and superficial white matter of the frontal, temporal, parietal, and occipital lobes will appear low SI on T2-weighted scans, similar to the adult pattern. The SI of these areas will however not be as low as the internal capsule, with that not occurring until 3 years of age. The deep white matter of the parietal lobes, surrounding the ventricular

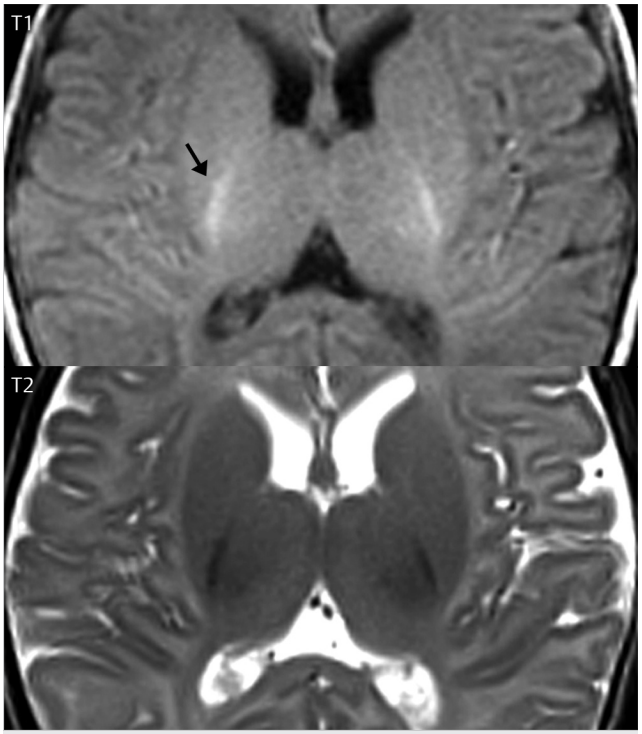

Fig. 1.7 Normal myelination in a newborn. At birth, the brain is principally not myelinated, with the appearance on MR strikingly different on both T1- and T2-weighted images when compared to the adult brain. Gray matter is predominantly of slightly higher signal intensity when compared to white matter on a T1-weighted scan in the newborn, with a principal indicator of early myelination being high signal intensity in the posterior limb of the internal capsule (*black arrow*).

trigones, is the last area to completely myelinate (the so-called zone of terminal myelination). Mild hyperintensity on T2-weighted scans in this region may persist up to 10 years of age.

1.1.5 Variants Involving the Septum Pellucidum

The septum pellucidum is a thin translucent plate, consisting of two laminae (leaves), that lies between the lateral ventricles. It extends from the corpus callosum superiorly to the fornix inferiorly. A cavum septum pellucidi is a common variant in which the two leaves are separated. This is a normal embryologic space, and is seen in all fetuses and premature infants. By 3 to 6 months of age only 15% of infants have a cavum septum pellucidi. The separation of leaves can persist into adulthood and as such is considered a normal variant.

A cavum septum vergae is also a normal embryologic space, like a cavum septum pellucidi but less common. It is essentially a posterior extension of a cavum septum pellucidi. It is seen as a midline cavity posterior to the columns of the fornix, which ends at the splenium of the corpus callosum. The internal cerebral veins lie inferiorly. When present in an adult, it is also considered to be a normal variant. The most common presentation is together with a cavum septum pellucidi, and in this instance the term cavum septum pellucidi et vergae (▶ Fig. 1.8) is used.

A cavum velum interpositum is a much less common variant, describing a cyst between the fornices superiorly and the roof

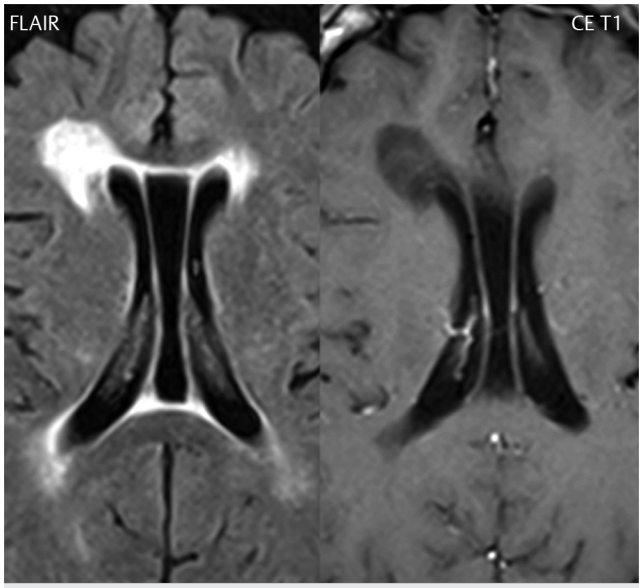

Fig. 1.8 Cavum septum pellucidi et vergae. In this patient with multiple sclerosis, and a prominent nonenhancing (chronic) right frontal plaque, the septum pellucidi are separated anteriorly, an extremely common normal variant. The division continues in this patient posteriorly, between the fornices, leading to a cavum septum pellucidi (anteriorly) and a cavum vergae (posteriorly).

of the third ventricle inferiorly. The internal cerebral veins lie within a cavum velum interpositum.

An absent septum pellucidum is rare, and almost always signifies major neurologic disease. It is associated with many congenital malformations, including septooptic dysplasia. An absent septum pellucidum can be an acquired abnormality, due to chronic hydrocephalus.

1.1.6 Physiological Calcification

The glomus portion of the choroid plexus, contained in the atria of the lateral ventricles, is the most frequent portion of the choroid plexus to calcify. Calcifications are usually globular and bilateral. Calcification and/or ossification is also commonly seen by CT in the falx (and less often in the pineal gland). These are all typically incidental findings. Because only dense, prominent calcification appears as low signal intensity on MR, calcification per se is less commonly visualized on MR. If the calcification is of sufficient size, it will however be seen on conventional MR. Ossification of the falx is well seen on MR due to visualization of the high signal intensity fat therein. Calcification and iron deposition are both dystrophic processes, and can occur together. Thus, sometimes what is seen as calcification on CT can be visualized as an abnormality on MR, but actually represents iron (hemosiderin) deposition.

1.1.7 Incidental Cystic Lesions

A pineal cyst is a common normal variant, and almost always asymptomatic. It is best visualized on thin section sagittal MR images. These are ovoid in shape, smoothly marginated, with a very thin wall, and rarely greater than 15 mm in diameter. The fluid therein will be homogeneous, with near CSF SI. On FLAIR,

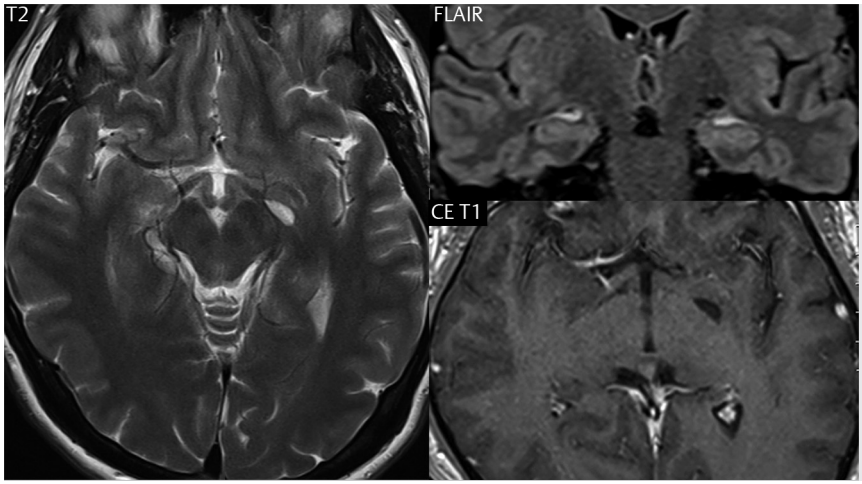

Fig. 1.9 Choroidal fissure cyst. These are considered a normal variant, and occur in the medial temporal lobe. They have CSF signal intensity on all MR pulse sequences, and expand slightly the choroidal fissure of the temporal lobe.

the cyst fluid will have slight high signal intensity. A thin uniform rim of contrast enhancement is common. Some large, but still asymptomatic, pineal cysts appear to have slight mass effect upon the adjacent colliculi.

Choroidal fissure cysts occur in the medial temporal lobe near the choroidal fissure (▶ Fig. 1.9). Their extra-axial location is easily confirmed on coronal images. Choroidal fissure cysts have a characteristic spindle shape when viewed in the sagittal plane.

1.1.8 Dilated Perivascular Spaces

The terms Virchow-Robin space and perivascular space are used interchangeably. This is a normal CSF space surrounding the perforating arteries entering the brain, and represents an invagination of the subarachnoid space. In the elderly, perivascular spaces may be more prominent. There are three common locations in which dilated perivascular spaces are seen. The first location is within the inferior third of the lentiform nucleus. In this instance the dilated spaces lie adjacent to the anterior commissure, following the course of the lenticulostriate arteries. Although usually less than 5 mm in diameter, larger dilated perivascular spaces can be seen in this location. These should be isodense on CT and isointense on MR to CSF. Differentiation can be difficult at times from chronic lacunar infarcts, with the latter the more common finding superiorly in the lentiform nucleus. The second common location for dilated perivascular spaces is within the white matter of the centrum semiovale. These follow the course of nutrient arteries, which lie along the white matter radiations. Thus, depending upon orientation relative to the slice, they may be seen either in cross-section or in plane, the latter as small radial structures. The third site, which is less common than the other two, is in the cerebral peduncle (near the substantia nigra). Although bilateral lesions may be seen here, typically the dilated perivascular space on one side is much larger than the other.

1.1.9 Other Incidental Lesions

Arachnoid granulations are small focal areas of arachnoid that protrude through the dura into the venous sinuses of the brain. CSF exits from the subarachnoid space via arachnoid granulations and enters the bloodstream, in part due to the normal higher pressure of CSF. These granulations also function as one-way valves. As MR has improved in terms of image quality and spatial resolution, visualization of arachnoid granulations within the transverse sinuses is not unusual. These should not be confused for venous thrombi.

A Tornwaldt cyst (▶ Fig. 1.10) is a common finding on MR of the brain, and is considered to be an incidental (benign) lesion. These vary in size, but are typically small. Tornwaldt cysts are thought to arise from the notochordal remnant, and occur in the posterior superior nasopharynx along the midline. They can be high signal intensity on T1-weighted scans, reflecting protein content.

Epidermoid cysts and small lipomas of the scalp are commonly encountered, incidentally. These entities have characteristic imaging appearances, on both CT and MR, and should be kept in mind when encountering a focal scalp lesion, due to their high incidence. The common small, painless lump under the skin seen incidentally on head CT is actually an epidermoid cyst, although often (incorrectly) termed “sebaceous cysts” by radiologists. The latter are much less common than epidermoid cysts, and affect the sebaceous glands, the oil glands in the skin.

1.2 Congenital Malformations

MR is the modality of choice for evaluation of all congenital malformations of the brain, with the exception of the craniosynostoses. In individual instances, some findings may be apparent on CT, with it thus being important to keep in mind the congenital malformations of the brain when interpreting CT.

1.2.1 Posterior Fossa Malformations

In a Chiari I malformation, there is displacement of the cerebellar tonsils > 5 mm below the level of the foramen magnum. This abnormality is not uncommon, and usually asymptomatic. On sagittal images the cerebellar tonsils are pointed or wedge-shaped (▶ Fig. 1.11). The fourth ventricle will be in normal position. Symptoms occur when there is obstruction of CSF flow through the foramen magnum. If there is crowding at the level of the foramen magnum, CSF flow studies can be obtained on MR to determine if the flow is abnormal and thus likely to contribute to symptoms (most frequently headache) (▶ Fig. 1.12). In symptomatic cases, there can be dilatation of the central canal of the

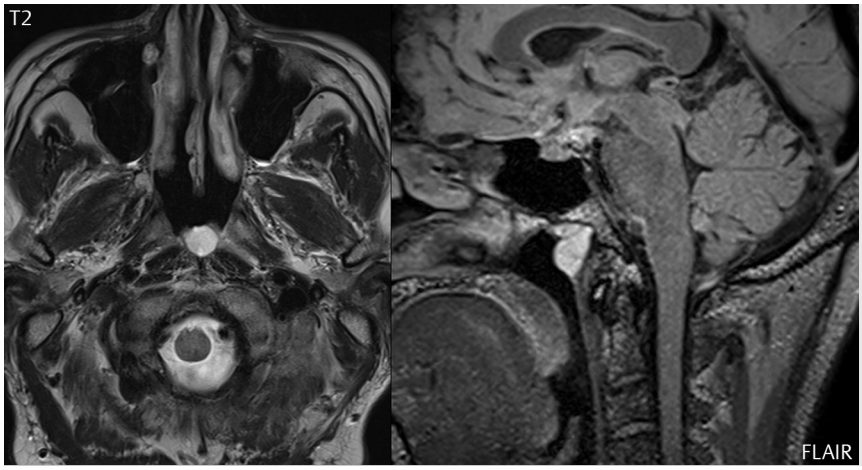

Fig. 1.10 Tornwaldt cyst. Axial T2-weighted and sagittal FLAIR scans reveal a well-circumscribed, round cyst along the midline in the upper posterior nasopharynx. This finding is considered incidental, of no clinical consequence.

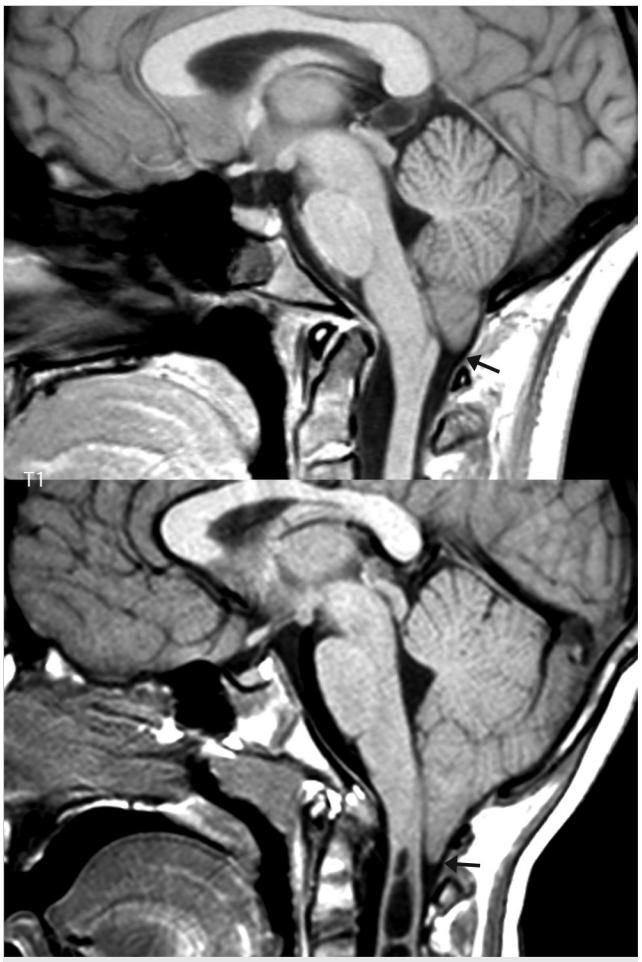

Fig. 1.11 Chiari I. In a Chiari I malformation, the cerebellar tonsils are pointed (*arrows*), and extend more inferiorly than normal, >5 mm below the level of the foramen magnum. Symptoms occur when normal CSF flow is prevented due to obstruction at the foramen magnum. Both patients in this instance have a paucity of CSF surrounding the cord at this level, and thus potentially could be symptomatic. The second patient however also demonstrates hydromyelia (dilatation of the central canal), consistent with altered CSF flow, with clinical symptomatology likely.

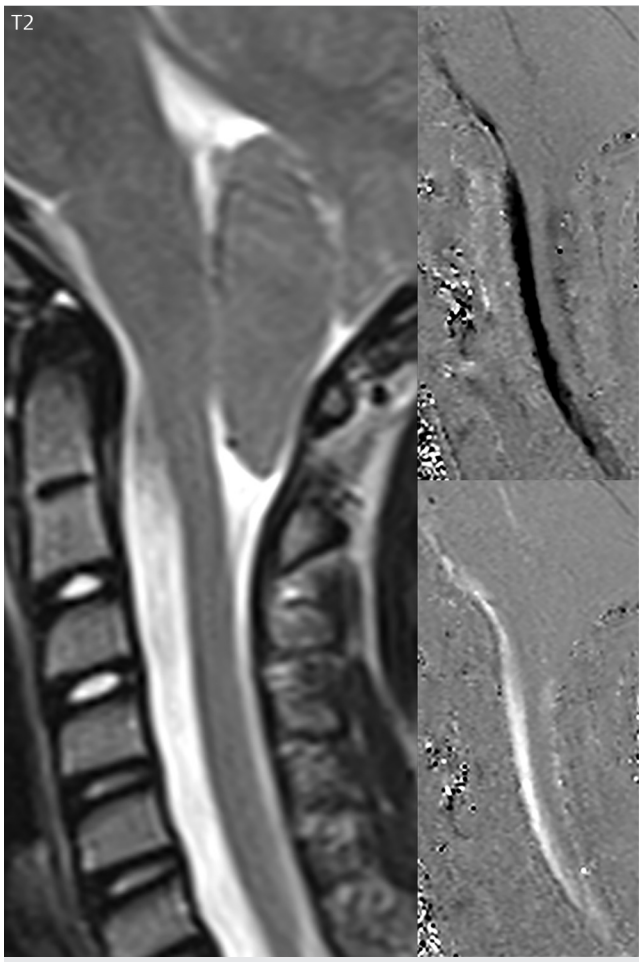

Fig. 1.12 Chiari I, with evaluation of CSF flow. The cerebellar tonsils are pointed, and extend below the C1 level. Note the normal configuration of the fourth ventricle. Phase contrast images at peak flow velocity in both the cranial and caudal directions are also illustrated. Flow is depicted as white or black, depending on direction, and is seen both anterior to the pons and anterior to the cord, establishing patency at the foramen magnum. An additional concordant finding is visualization of CSF anterior to the brainstem on the sagittal T2-weighted scan at that level.

spinal cord, specifically hydromyelia (more generally termed syringohydromyelia). Treatment is surgical, by suboccipital decompression with resection of the posterior arch of C1.

A Chiari I malformation is to be distinguished from tonsillar ectopia, specifically mild inferior displacement of the cerebellar tonsils seen in asymptomatic normal individuals. In this entity, the tonsils retain their normal globular configuration. In most normal individuals, the tonsils lie above the level of the foramen magnum, but they may lie as far as 5 mm below and still be normal.

The Chiari II malformation is a complex congenital brain anomaly, which involves principally the hindbrain (the medulla, pons, and cerebellum). Additional features involve the forebrain (the cerebral hemispheres, basal ganglia, and thalamic structures). In patients, a Chiari II malformation is associated with a neural tube closure defect in almost 100% of cases, usually a lumbosacral myelomeningocele. Characteristic features of a Chiari II malformation are subsequently described, not all features need be or are commonly present (▶ Fig. 1.13).

By definition, there will be a small posterior fossa with low insertion of the tentorium. The tentorial incisura may be widened, allowing the cerebellum to extensive superiorly, a "towering cerebellum." In this instance the folia of the cerebellum will have a vertical orientation. In a small number of cases the cerebellar hemispheres extend more anteriorly than normal, forming on an axial image the appearance of three bumps, the middle being that of the pons. The fourth ventricle is typically elongated (slitlike) and inferiorly displaced. A ballooned fourth ventricle is seen in 10%. Another defining feature is inferior displacement and elongation of the brainstem, tonsils, and vermis. The degree of displacement is often substantial. Cervicomedullary kinking, overlapping of the medulla and cervical cord, may occur. There may be an enlarged foramen magnum and upper cervical canal, accompanied by a smaller C1 ring, with resultant compression of displaced brainstem, tonsils, and vermis at this level. Cervical (and thoracic) syringohydromyelia is common. Obstructive hydrocephalus is usually present, with most patients shunted. Callosal dysgenesis (usually partial agenesis of the corpus callosum) is seen in 75%. Fusion of the colliculi, "tectal beaking," is seen in the majority. The frontal horns may have a characteristic inferior pointing seen on coronal images. The massa intermedia is typically large. There is often hypoplasia or fenestration of the falx, with interdigitation of cerebral gyri. Stenogyria (multiple small cerebral gyri) is common. A Chiari III malformation is rare, with features of the Chiari II malformation together with a low occipital or upper cervical encephalocele.

In a Dandy-Walker malformation, there are three primary features. The posterior fossa is large, with the confluence of the sinuses/torcula high in position. Additionally, there is a large posterior fossa cyst that communicates with the fourth ventricle anteriorly. The third defining feature is vermian and cerebellar hemisphere hypoplasia, which can be present to a varying degree (▶ Fig. 1.14). On sagittal images, the residual vermis may be rotated superiorly (counterclockwise). The occipital bone may be scalloped and thinned. Imaging in the sagittal plane is essential for definition of the structural abnormalities. There is a spectrum of severity of findings, and thus the additional use, in the past, of the terms Dandy-Walker continuum and Dandy-Walker variant. The term Dandy-Walker spectrum has also been suggested more recently, specifically including mega cisterna magna as the entity with the mildest findings.

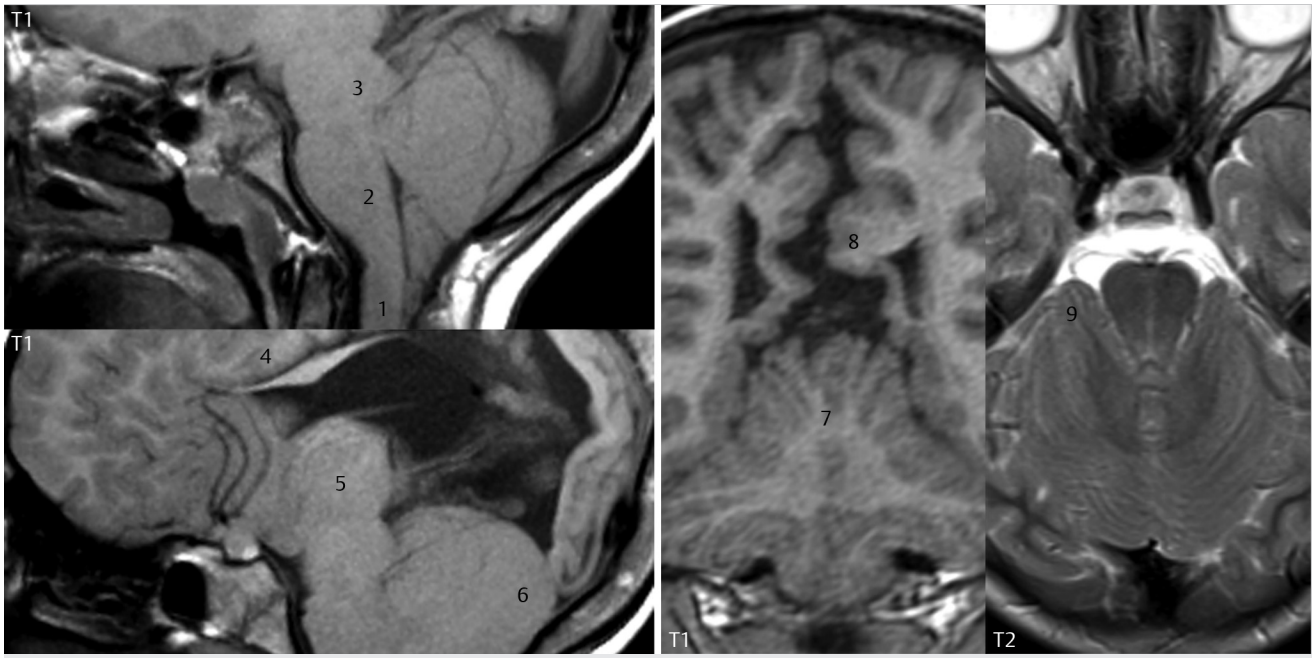

Fig. 1.13 Chiari II. This hindbrain dysgenesis has many characteristic features, not all of which will be present in the same patient. Illustrated are the peglike tonsillar herniation (1), a slitlike fourth ventricle (2), fusion of the colliculi with a beaklike appearance (3), partial agenesis of the corpus callosum (4), a large massa intermedia (5), low insertion of the tentorium (6), a towering appearance to the cerebellum with vertically oriented folia extending through a large tentorial incisura (7), partial agenesis of the falx with interdigitation of gyri (8), and anterior displacement of the cerebellar hemispheres relative to the pons (9).

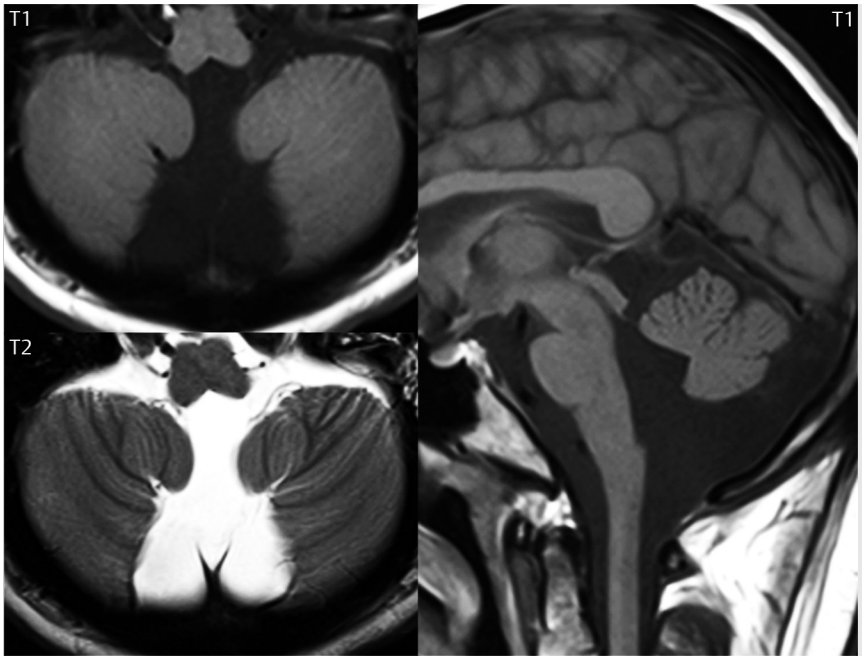

Fig. 1.14 Dandy-Walker malformation. There is dilatation of the fourth ventricle (which communicates with a posterior fossa cyst), hypoplasia of the inferior vermis, rotation of the vermis superiorly, and elevation of the torcula.

A mega cisterna magna is an enlarged CSF space posterior to the cerebellum, without mass effect, and with the cerebellar hemispheres, vermis and fourth ventricle specifically normal. These are common, and considered to be incidental findings. The primary differential diagnosis is a retrocerebellar (posterior fossa) arachnoid cyst. Although by definition there will be mild compression of the cerebellum, and scalloping of the calvarium may be present, most retrocerebellar arachnoid cysts are also asymptomatic. Like all arachnoid cysts, however, a discrete membrane separating the cyst from adjacent normal CSF is rarely seen on imaging. Retrocerebellar arachnoid cysts are most common along the midline. The size of the posterior fossa and position of the tentorium and straight sinus are usually normal, with the cerebellar vermis and hemispheres intact.

1.2.2 Cortical Malformations

Hemimegalencephaly is defined by hamartomatous overgrowth of a hemisphere. The lateral ventricle on the abnormal side is often large. Abnormalities of the brain on the side of involvement are common and include a thickened cortex and abnormal white matter signal intensity.

In heterotopic gray matter, there are displaced masses of gray matter, found anywhere from the embryologic site of development (periventricular) to the final destination after cell migration (cortical). The most common presentation is that of small focal regions of gray matter adjacent to the lateral ventricles (▶ Fig. 1.15). Important for diagnosis is that these small focal lesions are isointense to gray matter on all MR pulse sequences. The primary differential diagnostic consideration is tuberous sclerosis, specifically the subependymal nodules therein. The latter may demonstrate calcification, with the cortical involvement in tuberous sclerosis an additional differentiating feature. Less common forms of heterotopic gray matter include large nodular lesions and band heterotopia.

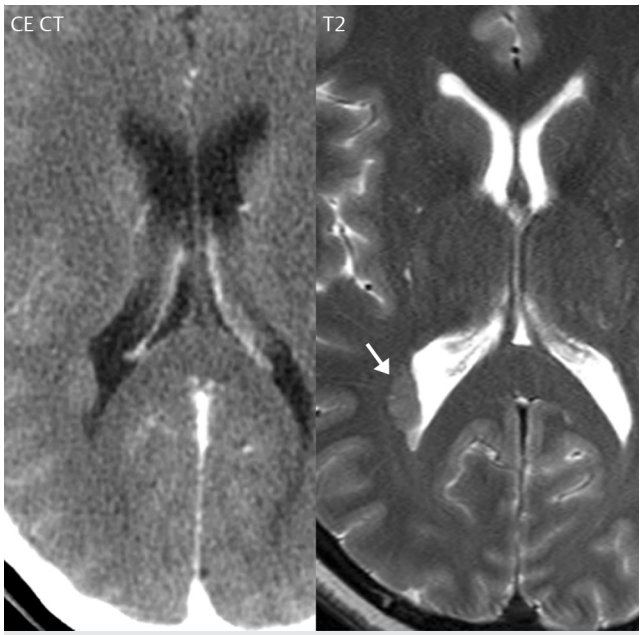

Fig. 1.15 Heterotopic gray matter. On CT, a small round lesion projects into the atrium of the lateral ventricle, with a suggestion that the attenuation is that of gray matter. On MR, this small heterotopic focus is isointense to and easily identified as gray matter. Isointensity to gray matter was confirmed on all pulse sequences (not shown).

The MR findings in focal cortical dysplasia (FCD) include blurring of the gray-white matter junction and an abnormal sulcal/gyral pattern (in a focal cortical distribution). In type 2, there is also focal cortical thickening (▶ Fig. 1.16). 10% of epilepsy patients have FCD. Of children less than 3 years of age, undergoing surgery for intractable epilepsy, 80% have FCD.

Lissencephaly type 1 or classic lissencephaly (previously known as the pachygyria-agyria complex) is a disorder of